Zero-temperature transition between antiferromagnetic and ferromagnetic states driven by varying chemical composition in hydrogenated $U_2(Ni_{1-x}Fe_x)_2Sn$

L. M. Sandratskii [1] and L. Havela [2]
[1]*Institute of Physics, Czech Academy of Sciences, 182 21 Prague, Czech Republic*
[2]*Faculty of Mathematics and Physics, Charles University, 12116 Prague, Czech Republic*

(Received 7 December 2021; revised 31 March 2022; accepted 1 April 2022; published 11 April 2022)

The experiment shows that hydrogenated $U_2(Ni_{1-x}Fe_x)_2Sn$ is antiferromagnetic for $x = 0$. With increasing Fe content, the Néel temperature decreases and tends to 0 K at $x \sim 20\%$. Further increase of x results in the ferromagnetism of the system. This paper suggests an explanation why the material that, from its chemical composition, is intermediate between antiferromagnet U_2Ni_2Sn and Pauli paramagnet U_2Fe_2Sn turns in the hydrogenated form to the ferromagnetic state—a state that is very unusual for the U compounds with the given crystal lattice. Our theoretical study is based on density functional theory (DFT) and DFT+U calculations. It begins with the calculation of U_2Ni_2Sn and U_2Fe_2Sn in their experimental lattices. Next, we show that for the lattice parameters of U_2Ni_2Sn, U_2Fe_2Sn becomes magnetic. To understand deeper the dependence of the magnetic states on the lattice parameters, we model quantum phase transitions in both parent systems. We find that a drastic difference of the 3*d*-5*f* hybridization in the two systems leads to fundamentally different types of the magnetic states. U_2Ni_2Sn has well-defined U atomic moments and can be mapped on the Heisenberg-type Hamiltonian of interacting U moments. In U_2Fe_2Sn, strong 5*f*-3*d* hybridization leads to both the Pauli paramagnetism for the equilibrium lattice and the simultaneous appearance of comparable in value U and Fe spin moments for larger lattice parameters. The presence of the Fe moments is shown to be essential for the magnetism of U_2Fe_2Sn, which imposes strong constraint on the magnetic structure of the U sublattice requesting it to be ferromagnetic. The established correlation between U and Fe spin moments is crucial for the explanation of the ferromagnetism of the hydrogenated $U_2(Ni_{1-x}Fe_x)_2Sn$.

DOI: 10.1103/PhysRevB.105.134411

I. INTRODUCTION

5*f* electron systems constitute an important branch of solid-state physics. They exhibit a wide variety of physical properties that are sensitive to the variation of temperature, pressure, magnetic field, and chemical composition [1–5]. Some of these properties are hidden order [6], unconventional superconductivity coexisting with antiferromagnetism and ferromagnetism [7], heavy electron masses [8,9], non-Fermi-liquid behavior [10], chiral magnetic structures [11], and quantum phase transitions [12]. Despite extensive research efforts devoted to U-based systems, many important questions remain open. The examples of the fundamental problems requiring further research attention, to mention a few, are the nature of the magnetic transformations in the magnetic field, and the origin of the heavy electron masses in the 5*f* systems. Further experimental and theoretical efforts are necessary to deepen our understanding of the electron processes governing the properties of the U-based materials.

This paper aims to shed light on the experimental finding of unexpected transformation of the magnetic ground state of a U-based system driven by the variation of the chemical composition of the 3*d* ligands. Recently, a number of studies considerably advanced the understanding of the nature of an unusual antiferromagnetic (AFM) structure and peculiar anisotropy properties of U_2Ni_2Sn [13–16]. On the other hand, it is known that U_2Fe_2Sn is a Pauli paramagnet without any signature of the presence of magnetic moments on either U or Fe sites. The experiment [17] shows that hydrogenated $U_2(Ni_{1-x}Fe_x)_2Sn$ is AFM for $x = 0$ with Néel temperature of 87 K. With increasing Fe content, the Néel temperature decreases, practically as a linear function of x, and tends to 0 K at $x \sim 20\%$. Further increase of x results in the ferromagnetism of the system. The crystal lattice in all cases remains of the Mo_2FeB_2 type (space group $p4/mbm$) (Fig. 1). Among a large number of the U compounds with this type of crystal lattice, all known magnetic compounds are AFM. One of the main goals of this paper is to understand why the material that appears as intermediate between antiferromagnet U_2Ni_2Sn and Pauli paramagnet U_2Fe_2Sn is ferromagnetic (FM)—a state that is very unusual for the U compounds with the given crystal lattice. Our main theoretical tool is density functional theory (DFT) calculations. They show good performance in the calculation of the magnetic states of the two parent systems, although these magnetic states are dramatically different. To corroborate our conclusions, we also perform calculations with the DFT+U method.

Our theoretical study begins with the discussion of U_2Ni_2Sn and U_2Fe_2Sn in their experimental lattices. Then we present the results showing that for the lattice parameters of U_2Ni_2Sn, U_2Fe_2Sn becomes magnetic. To further investigate the dependence of the magnetic states on the lattice parameters we study for the parent systems the transition between magnetic and nonmagnetic (NM) states caused by

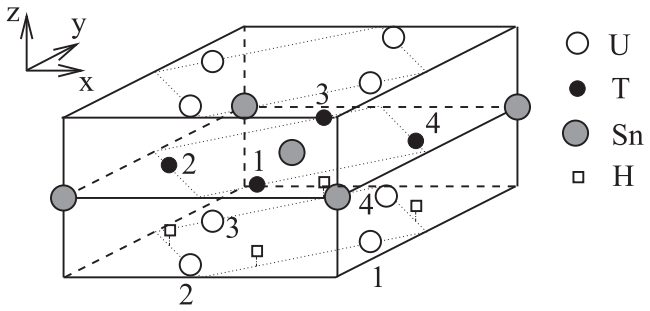

FIG. 1. Unit cell of the crystal structure of the systems considered in the paper. *T* atoms are either Ni or Fe. Numbering of the U and *T* atoms is used in Table II.

the variation of the lattice parameters. We demonstrate that the difference of the 3*d*-5*f* hybridization in the two systems leads to a fundamentally different character of the magnetic states. U_2Ni_2Sn has well-defined U atomic moments whereas the induced Ni moments, if present, are very small. In U_2Fe_2Sn, strong U 5*f*-Fe 3*d* hybridization is responsible for the Pauli paramagnetism for the equilibrium lattice. For larger lattice parameters, the calculations reveal a simultaneous appearance of comparable in value and opposite in direction spin moments of the U and Fe atoms, properties that cannot be understood without accounting for the character of the U-Fe hybridization. We show that the magnetism of U_2Fe_2Sn depends on the presence of the Fe moments. This feature imposes the constraint on the magnetic structure of the U sublattice: it must be FM. We corroborate our findings performing DFT+U calculations using different double-counting terms and drawing a conclusion in favor of the around mean-field (AMF) type of the term. Based on the revealed importance of the Fe moments for the stabilization of the magnetism of the U sublattice,we discuss the origin of the ferromagnetism of the hydrogenated $U_2(Ni_{1-x}Fe_x)_2Sn$ obtained in both experiment and our calculations.

The transformation of the ground magnetic state driven by the variation of the chemical composition as a control parameter belongs to the class of quantum phase transitions (QPTs) [12,18]. QPTs are an active field of modern condensed-matter physics. Close to the critical value of the control parameter, the system experiences strong nonthermal fluctuations, leading to unusual physical properties such as non-Fermi-liquid behavior. The DFT and DFT+U methods employed in this paper do not allow us to take into account these quantum fluctuations. Therefore, the dynamics of the QPT in the region of concentration x around the critical concentration x_{cr} is not the topic of this paper. Further efforts are needed to address this problem.

The paper is organized as follows. In Sec. II, we present our calculation technique. Section III is devoted to the results of the calculations and their interpretation. In Sec. IV, we formulate our conclusions.

II. DETAILS OF CALCULATIONS

A. Method of calculations

The main part of the calculations is performed with the augmented spherical wave (ASW) method [19–21] and the generalized gradient approximation (GGA) [22] exchange-correlation potential. The spin-orbit coupling (SOC) is self-consistently included into consideration. The operator of the SOC is taken in the form [23]

$$\mathbf{H}_{\rm so} = \frac{1}{(2c)^2}\frac{1}{r}\left[\begin{pmatrix} \frac{1}{M_+^2}\frac{dV^+}{dr} & 0 \\ 0 & \frac{1}{M_-^2}\frac{dV^-}{dr}\end{pmatrix}\sigma_z\hat{l}_z + \frac{1}{M_{av}^2}\frac{dV^{av}}{dr}(\sigma_x\hat{l}_x+\sigma_y\hat{l}_y)\right] \quad (1)$$

where V^+ and V^- are spin-up and spin-down electron potentials,

$$V^{av} = \tfrac{1}{2}(V^+ + V^-) \quad (2)$$

and

$$M_\alpha = \tfrac{1}{2}\left(1 - \tfrac{1}{c^2}V^\alpha\right) \quad , \alpha = av, +, -. \quad (3)$$

$\sigma_x, \sigma_y, \sigma_z$ are the Pauli matrices and $\hat{l}_x, \hat{l}_y, \hat{l}_z$ are the operators of the components of the orbital momentum, r is the distance from the center of atomic sphere, c is the light velocity. The SOC is taken into account for all atoms.

We calculate the z components of spin m_s^ν and orbital m_o^ν moments of the νth atom as

$$m_s^\nu = \sum_{\mathbf{k}n}^{\rm occ}\int_{\Omega_\nu}\psi_{\mathbf{k}n}^\dagger\sigma_z\psi_{\mathbf{k}n}d\mathbf{r}, \quad (4)$$

$$m_o^\nu = \sum_{\mathbf{k}n}^{\rm occ}\int_{\Omega_\nu}\psi_{\mathbf{k}n}^\dagger\hat{l}_z\psi_{\mathbf{k}n}d\mathbf{r}, \quad (5)$$

where $\psi_{\mathbf{k}n}$ is the wave function of the Kohn-Sham state corresponding to wave vector $\mathbf{k}$ and band index n. The sum is taken over occupied states. The integrals are carried out over νth atomic sphere.

In the ASW method, the wave functions of the crystal electrons are presented as linear combinations of atomic basis functions. These basis functions have quantum numbers l, m, σ, which is a convenient choice when dealing with the SOC added to the scalar relativistic Schrödinger equation. (In the methods dealing with the Dirac equation, the basis functions characterized by quantum numbers of total angular momentum j and its projection j_z are preferable.) The crystal electron states appear as mixtures of the atomic orbitals with different quantum numbers. According to Eqs. (4) and (5), the calculated atomic spin and orbital moments are the expectation values of the corresponding operators and not the eigenvalues of those operators. The question of making a choice between *J*-*J* and *L*-*S* couplings important in the theory of angular momentum of isolated atoms does not arise in the DFT calculations.

Strong SOC of the U 5*f* electrons leads to large values of the atomic orbital moments that reflects the fact that the contribution of the basis functions with quantum numbers (m, σ) and $(-m, \sigma)$ to the crystal electron states are different. In a magnetic crystal, the lowest in energy electron states of U 5*f* character have a leading contribution of atomic basis functions with $\sigma{=}1/2$ and $m{=}{-}3$, whereas for the highest in energy states, the main contribution comes from the atomic orbitals with $\sigma{=}{-}1/2$ and $m = 3$. Obviously, the latter states lie above Fermi energy and are unoccupied.

In the calculations, we used $l_{\max} = 4$ for the U atoms and $l_{\max} = 3$ for Fe, Ni, and Sn atoms. The **k** mesh in the Brillouin zone (BZ) was up to $20 \times 20 \times 20$. The convergence criterion was the energy differences of various magnetic states of the system to be below 1 meV.

B. Direction of atomic moments with respect to crystal lattice

One of the characteristic features of the U compounds is a very large magnetic anisotropy. Therefore, the selection of the directions of the atomic moments with respect to the crystal lattice in the first-principles calculations of the U-based magnets is an important aspect to consider. The experimental information about the magnetic anisotropy of the studied systems is by far not complete and requires further intensive efforts. At present, it is known that in the parent U_2Ni_2Sn the easy axis is parallel to the z axis [13]. The energy of the magnetic anisotropy is as large as 14.6 eV per U atom. Remarkably, the hydrogenation of U_2Ni_2Sn was reported to change the anisotropy to the basal-plane type [24]. The theoretical explanation of the dramatic effect of hydrogenation was suggested in Ref. [15] and based on accounting for the disturbance of local symmetry by the H atoms. The only further available experimental information is a recent measurement on the monocrystal of $U_2(Ni_{0.5}Fe_{0.5})_2Sn$ that reveals the z axis as an easy axis [25]. To limit the amount of calculations, we perform them with atomic moments collinear to the z axis. In the case of $U_2(Ni_{0.5}Fe_{0}.5)_2Sn$, we carried out an additional calculation with moments parallel to the basal plane to verify that the conclusions of our study also remain intact in this case. A systematic study of the anisotropy properties of the $U_2(Ni_{1-x}Fe_x)_2Sn$ systems remains a task for future investigations.

C. DFT+U calculations

The U $5f$ electron correlations in the U compounds cannot be fully accounted for with the standard DFT approaches as local density approximation (LDA) or GGA. On the other hand, the extent of the localization of the $5f$ electrons and, respectively, the strength of the electron correlations varies widely from system to system, extending from very strong in, e.g., UPd_3 [26] to relatively weak in, e.g., $U_2Ni_{21}B_6$ [27]. Even different properties of the same system can require different approaches to the treatment of the electron system. For instance, the spectroscopic experiments and such phenomena as superconductivity or dynamic fluctuations cannot be addressed in standard DFT calculations. However, the DFT methods are useful and show good performance in the description of the ground-state magnetic properties of moderately correlated U compounds. The problem considered in this paper belongs to those where DFT provides valuable physical insight. An important argument supporting this conclusion is the fact that DFT successfully describes the very different magnetic ground states of the parent compounds.

To corroborate the conclusions following from the DFT calculations, we performed some calculations with the DFT+U method [28]. This method is a widely employed tool to account for the electron correlations beyond DFT. We use the flavor of the method suggested by Dudarev *et al.* [29]. The main idea of the DFT+U approach is to make the electron potential orbital dependent, which is achieved by making the energy functional dependent on the occupation matrix of the correlated electrons. There is an important aspect of the DFT+U method that is relevant to our investigation. The DFT+U energy functional includes a so-called double-counting term whose purpose is to subtract the part of the energy already accounted for by the DFT functional. This term cannot be uniquely established. There are two widely used forms of the double-counting term that are usually referred to as the fully localized limit (FLL) and AMF [30]. The FLL correction to the electron potential in Dudarev *et al*'s. flavor of the DFT+U method has the following form:

$$V_{m,m'} = -U\left(n_{m,m'} - \tfrac{1}{2}\delta_{m,m'}\right), \tag{6}$$

whereas the AMF correction is

$$V_{m,m'} = -U(n_{m,m'} - \langle n\rangle\delta_{m,m'}). \tag{7}$$

Here n is the orbital density matrix of the correlated atomic states. The diagonal elements $n_{m,m}$ of the orbital density matrix give the occupations of the corresponding m orbitals. $\langle n\rangle$ is the average value of $n_{m,m}$. Examples of the implementation of the n matrix calculation within the DFT methods can be found in Refs. [31,32].

In both cases of the double-counting treatment [Eqs. (6) and (7)], stronger occupied orbitals tend to decrease their energy whereas less occupied orbitals tend to increase their energy. In the self-consistent calculations, this process can lead to the insulating gap between correlated states, which is crucial for the description of the Mott-Hubbard insulators [33,34]. It is also useful as a tool to enhance the value of the orbital moment that is often underestimated in the DFT calculations [35,36]. However, in detail the processes are different for the two versions of the double-counting corrections. In the FLL case, the orbitals that are more than half occupied decrease their energy whereas the orbitals that are less than half occupied increase it. In the AMF case, the direction and values of the energy shift, depending on the comparison of the occupation of the orbital to the average occupation of all orbitals. This means that if all correlated orbitals are equally occupied, no change of the electronic structure takes place. It was suggested that the AMF form of the double-counting term provides better performance in the case of moderately correlated systems [30,37]. For instance, in FeAl, the AMF term leads, in agreement with experiment, to the NM ground state whereas both DFT and DFT+U with the FLL double-counting term result in a magnetic ground state [37].

We performed calculations with both types of the double-counting terms and different values of the Hubbard parameter U. We report on the results of these calculations in Sec. III D.

III. RESULTS OF CALCULATIONS

A. U_2Ni_2Sn and U_2Fe_2Sn in their experimental lattices

To systematically build up a consistent physical picture of the processes leading to the transition from antiferromagnetism of U_2Ni_2Sn to ferromagnetism of $U_2(Ni_{1-x}Fe_x)_2Sn$, we begin with the comparison of the density of states (DOS) of NM unhydrogenated U_2Ni_2Sn and U_2Fe_2Sn in their experimental lattices [Figs. 2(a) and 3(a)]. Lattice parameters used in the calculations are collected in Table I.

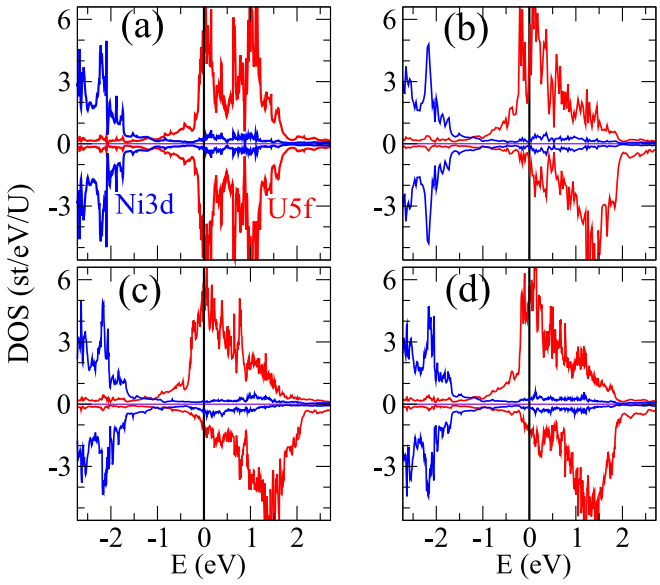

FIG. 2. Spin-resolved partial U 5*f* and Ni 3*d* DOSs of U_2Ni_2Sn. (a) Nonmagnetic state. (b) AFM-G state. (c) FM state. (d) AFM-A state. The curves above (below) the abscissa axis give spin-up (spin-down) DOS. The energy origin is at the Fermi level. Notations for magnetic structures is according to Fig. 4.

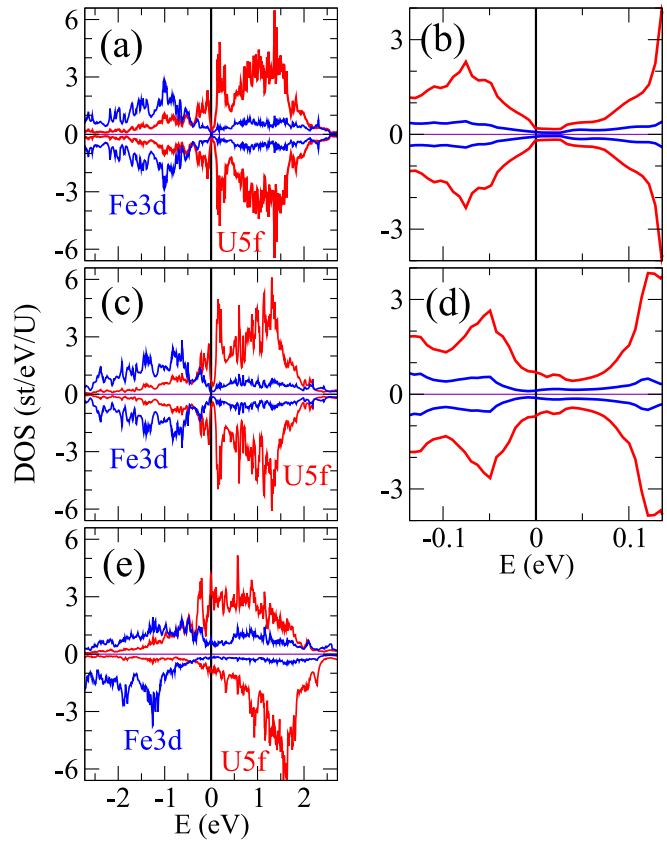

FIG. 3. Spin-resolved partial U 5*f* and Fe 3*d* DOSs of U_2Fe_2Sn. (a) Nonmagnetic state for the experimental lattice (b) The same as (a) but zoomed in the energy region around the Fermi energy. (c) Nonmagnetic state for the U_2Ni_2Sn lattice. (d) The same as (c) but zoomed in the energy region around the Fermi energy. (e) Ferromagnetic state for the U_2Ni_2Sn lattice. In the presentation of the spin-projected partial DOSs in the ferromagnetic case, we use the same direction of the spin-quantization axis parallel to the direction of the U spin moment for both U and Fe atoms.

The Ni 3*d* states in U_2Ni_2Sn lie distinctly below the Fermi energy (E_F) and are almost completely filled [Fig. 2(a)]. On the contrary, the U 5*f* states of U_2Ni_2Sn are richly present at E_F, resulting in high U 5*f* DOS at E_F. According to the Stoner criterion, high DOS at the Fermi energy is a factor contributing to the destabilization of the NM state with respect to the formation of a magnetic state. The Stoner criterion reflects the competition between the reduction of the electron exchange energy through the spin polarization of the electron density and an accompanying increase of the electron kinetic energy [38]. Indeed, our spin-polarized calculations resulted in self-consistent magnetic states of the system. We performed calculations [14] for the magnetic states with different relative orientations of the U atomic moments (Fig. 4). In all cases, we obtained self-consistent magnetic states with energies lower than the energy of the NM state. The U spin moment varies in the range 2.15–2.34 μ_B, the Ni moments are very small if not zero by symmetry. The fact that the self-consistent magnetic state can be obtained for different magnetic configurations and that the value of the U moment varies only weakly with the change of the magnetic configuration indicates the presence of well-defined U atomic moments [14]. We emphasize that these well-defined U atomic moments are formed by the electron states treated as itinerant. This type of duality in the properties of the open shell electrons of transition metals has been discussed many years ago in the framework of the fluctuation theory of itinerant magnets (see, e.g., Ref. [39]).

In Fig. 4, the formation of the well-defined atomic U moment is reflected in the similarity of the DOS of differ-

TABLE I. Lattice parameters used in the calculations (in Å).

	a	c
U_2Ni_2Sn	7.249	3.672
U_2Fe_2Sn	7.296	3.446
$U_2(Ni_{0.75}Fe_{0.25})_2Sn$-$H_2$	7.489	3.704
$U_2(Ni_{0.5}Fe_{0.5})_2Sn$-$H_2$	7.503	3.653
$U_2(Ni_{0.25}Fe_{0.75})_2Sn$-$H_2$	7.527	3.596
U_2Fe_2Sn-H_2	7.525	3.549

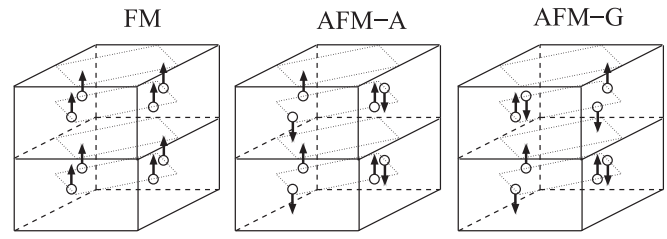

FIG. 4. Magnetic structures considered in the paper. Two layers of the U atoms are shown. FM: Ferromagnetic structure. AFM-A: Antiferromagnetic structure with identical U layers. AFM-G: Antiferromagnetic structure with oppositely directed magnetic moments of the corresponding atoms of the two neighboring layers.

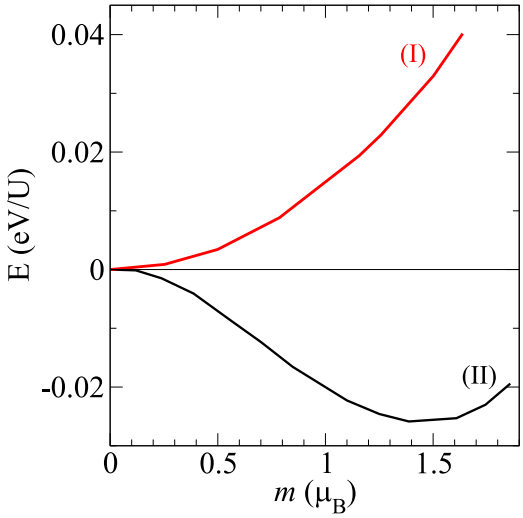

FIG. 5. Energy as the function of the U spin moment for U_2Fe_2Sn. Curve (I) is obtained for the experimental lattice of U_2Fe_2Sn. Curve (II) is obtained for the experimental lattice of U_2Ni_2Sn.

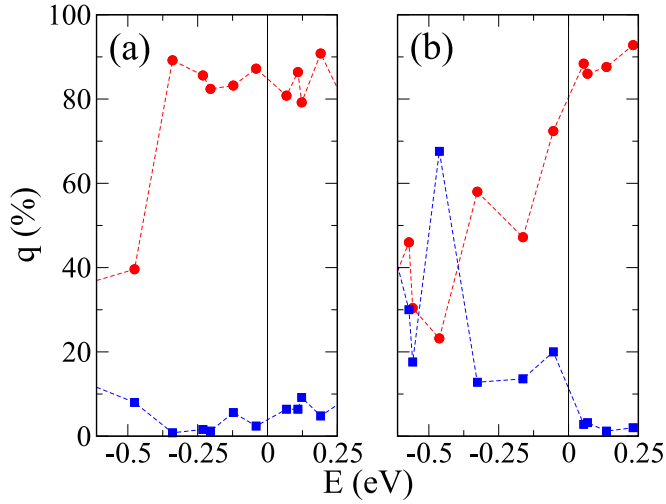

FIG. 6. The contribution in percent of the U 5*f* (read circles) and Fe 3*d* (blue squares) orbitals in the electron states at Γ point of the BZ of nonmagnetic U_2Ni_2Sn [panel (a)] and U_2Fe_2Sn [panel (b)]. The energy origin is at the Fermi energy. The lines are for visual help only.

ent magnetic configuration [Figs 4(b)–4(d)] and their strong difference from the NM DOS [Fig. 4(a)]. This is the consequence of the weak hybridization of the U 5*f* and Ni 3*d* states. Since the U 5*f* states do not hybridize with the Ni 3*d* states, they preserve to a large degree their atomiclike character and their spin polarization is governed by the intraatomic exchange interaction leading to large in value and weakly configuration-dependent U spin moments. The presence of the well-defined atomic moments allows the mapping of U_2Ni_2Sn on the Heisenberg-type model Hamiltonian of interacting U atomic moments [14].

In U_2Fe_2Sn, both U 5*f* and Fe 3*d* states are present close to E_F [Fig. 3(a)]. They hybridize strongly with each other, showing a common structure of peaks and dips of the partial atomic DOS. Importantly, the position of E_F is at the minimum of the DOS. As discussed above, the low DOS at E_F is known to contribute to the stabilization of the NM state with respect to the formation of the FM state. Indeed, in U_2Fe_2Sn the calculated ground state is NM: The calculations started with magnetic U atoms converge to the state with vanished atomic moments. Using the idea of a fixed spin moment method [40], we performed calculations with magnetic field applied to the U spin moments and obtained $E(m)$ curve [curve (I) in Fig. 5] where m is the value of the U spin moment. The shape of the $E(m)$ curve confirms that in U_2Fe_2Sn the NM state is the only stable state. There is no signature of a metastable state with a local energy minimum at a nonzero m.

Before proceeding further, we would like to give an additional comment on the difference in the hybridization of the U 5*f* states with the 3*d* states of Ni and Fe. Because of high filling of the Ni 3*d* shell (the estimations give ∼8.6 3*d* electrons per Ni atomic sphere), the electron states with large Ni 3*d* contribution lie distinctly below E_F. This position of the Ni 3*d* states leads to a weak contribution of the Ni 3*d* orbitals to the electron states lying close to E_F and contain a large portion of the U 5*f* electrons. In contrast to Ni, the number of the Fe 3*d* electrons per atomic sphere is ∼6.6. In this case, both Fe 3*d* and U 5*f* orbitals contribute to the crystal states lying about E_F. (The calculated number of the U 5*f* electrons per U atom is close to 3).

The above discussion of the *f*-*d* hybridization is based on the consideration of the DOS that are cumulative characteristics obtained by the integration over the BZ. It is instructive, however, to look closer at the individual electron states where the actual process of the hybridization takes place. In Fig. 6, we present, as an example, the contributions of the U 5*f* and *T* 3*d* atomic orbitals for the states at point Γ of the BZ. We consider the states lying close to the Fermi energy. The difference between U_2Ni_2Sn and U_2Fe_2Sn is clearly seen: While the U_2Ni_2Sn states just below E_F are of almost pure U 5*f* origin, the U_2Fe_2Sn states in this energy region are strong mixtures of the U 5*f* and Fe 3*d* contributions. The values of the partial U and Fe contributions vary substantially from state to state, reflecting a complex process of the formation of the electron states in the U-based intermetallic compounds.

Because of the weakness of the hybridization of the U 5*f* states with the Ni 3*d* orbitals, the corresponding crystal states are predominantly localized on the U atoms. On the other hand, the hybridization of the U 5*f* with Fe 3*d* orbitals results in the delocalization of the states. These processes play an important role in the formation of the magnetic properties of both systems. The complexity of the hybridization processes in different electronic states precluded us from attempting to quantify them by a single parameter characterizing a U-based material. An example of performing and employing such a parametrization for a series of U compounds can be found in an early work by Endstra *et al.* [41].

B. U_2Fe_2Sn in the lattice of U_2Ni_2Sn

An important aspect of our study is the dependence of the magnetic state on the interatomic distances. The U_2Ni_2Sn and U_2Fe_2Sn have the same crystal lattice but considerably different lattice parameters (see Table I). The hydrogen

absorption increases lattice parameters which should be taken into account in the calculation of the hydrogenated systems.

The relation between interatomic distances and magnetism of the U compounds has attracted attention for many decades. An empirical criterion known as the Hill criterion [42] implies that a U compound is magnetic if the shortest U-U distance is above 3.5 Å. As the physical basis of the criterion, it was suggested that below critical Hill distance a direct overlap of the U 5*f* states takes place leading to broadening of the U 5*f* energy bands and vanishing of the magnetism. It is now understood that this explanation of the empirical relationship reflected in the Hill's criterion is an oversimplification of the underlying physics since the hybridization of the U 5*f* states with the states of other atoms plays an important role and must be taken into account (see, e.g., a recent comment in Ref. [43]).

To get insight into the dependence of the magnetic state of U_2Fe_2Sn on the lattice parameters, we performed calculations of U_2Fe_2Sn with the U_2Ni_2Sn lattice. The general structure of the NM DOS [Fig. 3(c)] remained unchanged [compare Figs. 3(c) and 3(a)]. However, quantitative changes are clearly seen. Although E_F is still in the region of the local minimum of the DOS, this minimum is less pronounced [Fig. 3(d)]. In general, increasing the interatomic distance is expected to lead to narrower electron bands. Respectively, narrower DOS peaks and deeper minima between them can be expected. However, this argumentation cannot be applied if the minimum between the DOS peaks is the result of the interatomic hybridization of the electronic states. The hybridization leads to the formation of bonding and antibonding states that effectively repel each other. Since increased interatomic distance reduces interatomic hybridization, the trend to the formation of the minimum between bonding and antibonding peaks becomes less pronounced. This is the process we observe in the case of U_2Fe_2Sn. According to the Stoner picture, an increased DOS at E_F influences the competition between exchange energy and kinetic energy and, respectively, the competition between energies of the magnetic and NM states (of U_2Fe_2Sn) in favor of the magnetic state. (Obviously, such a change of the electronic structure influences the energy competition between magnetic and NM states of U_2Fe_2Sn.) Indeed, the iterations started with ferromagnetically ordered U moments converge in this case to the magnetic U_2Fe_2Sn [Fig. 3(e)]. The calculated $E(m)$ curve has now the minimum [curve (II) in Fig. 5] at nonzero m and the maximum at the NM state $m = 0$, in sharp contrast to the $E(m)$ curve obtained for the experimental U_2Fe_2Sn lattice [curve (I) in Fig. 5].

A closer look at the properties of the magnetic U_2Fe_2Sn reveals a number of important features. First, the values of the U and Fe spin moments are comparable. This feature is in strong contrast to the U_2Ni_2Sn case where the Ni spin moment is much smaller than the U spin moment. Second, the direction of the Fe spin moments is opposite to the direction of the U spin moments. Therefore, although the U magnetic structure is FM, the spin structure of the system as a whole is ferrimagnetic. In the DOS [Fig. 3(e)], we see that due to a large Fe spin moment, the spin-down Fe states moved strongly toward lower energies whereas the spin-down U 5*f* states moved to higher energies lying now above E_F [44]. Because of the spin polarization of the U and Fe states, the energy distance between the spin-down U and Fe states increases leading to decreased U 5*f*-Fe 3*d* hybridization in the spin-down channel. Obviously, strong decrease of the energy of the occupied spin-down states contributes to the energy competition favoring the formation of the magnetic state.

The attempts to obtain the magnetic U_2Fe_2Sn without Fe moments lead to vanishing U moments. This result was achieved in several types of calculations: First, the Fe moments were constrained to be zero and a large spin moment of $\sim 2\ \mu_B$ was created on the U atoms at the beginning of the iterations. The self-consistent calculation resulted in the nonmagnetic state. Second, in the calculation where the U magnetic structure was assumed AFM, the U moments vanished since oppositely directed U moments prohibit the formation of the induced Fe moments. Third, the attempt to obtain the Fe spin moments parallel to the U spin moments resulted in vanishing of all atomic moments. These calculations show that the presence of the Fe moments and their orientation are essential for the magnetism of U_2Fe_2Sn.

Inspection of the DOS depicted in Fig. 3 allows us to suggest an explanation why the opposite direction of the Fe spin moments with respect to the U spin moments is important for obtaining magnetic U_2Fe_2Sn. The state with parallel U and Fe moments would result in a shift of the spin-up DOS of the nonmagnetic U_2Fe_2Sn [Fig. 3(c)] to lower energies and simultaneous shift of the spin-down DOS to higher energies. The general structure of the DOS would be preserved. Since the Fermi level of the nonmagnetic U_2Fe_2Sn [Fig. 3(c)] is at the dip of the DOS, the shifts of the DOS would lead to the increase of the DOS at E_F for both spin-up and spin-down channels. Such changes of the DOS are not expected to lead to an energetically more stable state of the system. On the other hand, opposite directions of the U and Fe spin moments result in a strong change of the structure of the NM DOS [Fig. 3(e)]. In the global spin-down channel, the Fe 3*d* states move downward while the U 5*f* states move upward. These opposite movements caused by the intra-atomic exchange interactions of both atoms lead to reduced DOS at E_F and decreased hybridization of the U 5*f* and Fe 3*d* states in the spin-down channel. As a result, the system obtains a self-consistent state where the occupied Fe 3*d* states are strongly shifted to lower energies, making this state of the system energetically preferable compared to the NM one. Because of decreased U-Fe hybridization, the role of the intra-atomic exchange interaction in the Fe atoms increases, leading to the values of the Fe moments comparable with the U spin moments. In contrast to U_2Ni_2Sn, U_2Fe_2Sn cannot be described in terms of the well-formed atomic moments since the attempt to obtain the magnetic state with different relative orientation of the atomic moments leads to their vanishing.

C. Magnetic QPT in U_2Ni_2Sn and U_2Fe_2Sn caused by the variation of the lattice parameter.

To obtain a more detailed view of the dependence of the magnetic properties of U_2Ni_2Sn and U_2Fe_2Sn on the interatomic distances, we performed calculations for the sets of the lattice parameters, paying special attention to the region where the transition between magnetic and NM states takes place.

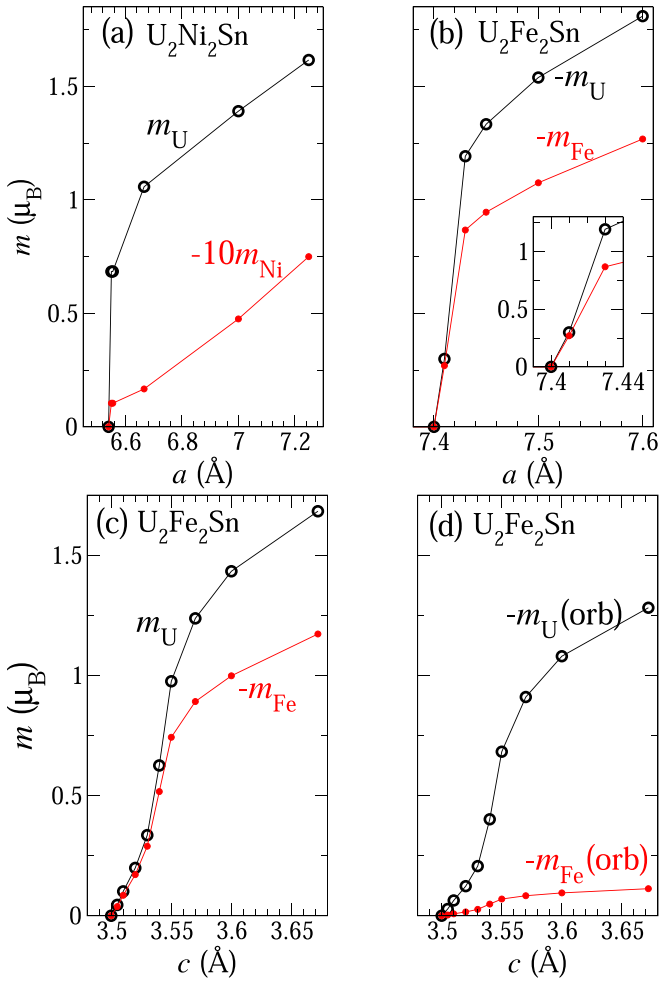

FIG. 7. Investigation of the quantum phase transition between FM and NM caused by the variation of the lattice parameters. Negative values of the moments mean that their directions are opposite to the direction of the U spin moment. (a) U_2Ni_2Sn. Spin moments of U and Ni as functions of lattice parameter a. The value of the Ni moment is multiplied by 10. (b) U_2Fe_2Sn. Spin moments of U and Fe as the functions of lattice parameter a. Inset: Zooming in the region of the phase transition. (c) U_2Fe_2Sn. Spin moments of U and Fe as functions of lattice parameter c. (d) U_2Fe_2Sn. Orbital moments of U and Fe as functions of lattice parameter c.

We will consider separately the variation of the a and c lattice parameters and begin with U_2Ni_2Sn. In the equilibrium state, the shortest distance between the U atoms along the c axis is 3.672 Å. The shortest distance in the basal plane is 3.572 Å. Both values are above the Hill limit. The reduction of the c parameter to 3.2 Å that is distinctly below the Hill limit does not lead to the transformation of the FM state to the NM state. The FM is still 2.6 meV/U lower in energy than the NM state. This energy difference is expectantly smaller than the corresponding difference of 40.5 meV/U for the experimental lattice.

In Fig. 7(a), we show atomic moments of U and Ni as the functions of the lattice parameter a calculated for the fixed experimental parameter c. At critical value $a_{cr} \sim 6.54$ Å, the system becomes NM. This value of the a parameter corresponds to the shortest in-plane U–U distance of 3.435 Å, somewhat below the Hill limit. In the magnetic state, for all a values the U spin moment is much larger than the Ni spin moment. In numerical calculations, it is difficult to establish if the transition is truly discontinuous. However, it is obvious that the transition is at least very close to discontinuity.

In Figs. 7(b)–7(d), we show the results for U_2Fe_2Sn. Figure 7(b) presents the U and Fe spin moments obtained in the calculations where parameter c is kept at the experimental value while the a parameter is varied. In Figs. 7(c) and 7(d), we present spin and orbital moments obtained in the calculations where the experimental parameter a is kept unchanged and the parameter c is varied. In both cases, we obtain the transition of the experimental NM state to the FM state. For fixed c, the transition takes place at $a = 7.4$ Å corresponding to the shortest in-plane U-U distance of 3.550 Å, somewhat above the Hill limit. For fixed a, the transition to FM takes place at $c = 3.5$ Å, precisely at the Hill's critical value.

Importantly, we again obtained strong qualitative difference in the properties of U_2Ni_2Sn and U_2Fe_2Sn. In the case of U_2Fe_2Sn, the transition is continuous. Near the transition point from the magnetic side, the values of the U and Fe spin moments are very close to each other [Fig. 7(c)]. This means that we actually deal not with a FM spin structure but with almost perfectly compensated spin ferrimagnet. We also notice that in U_2Fe_2Sn, the U orbital moment is smaller than the U spin moment [Figs. 7(c) and 7(d)]. This is rather unusual for the U atoms in the U compounds and is a signature of a stronger delocalization of the U 5f states than in most of the compounds.

D. DFT+U calculations

Next we report on the calculations with the DFT+U method. Our calculations have shown that the FLL correction to the electron potential [Eq. (6)] gives strong moment enhancement and overestimates the trend to the ferromagnetism in U_2Fe_2Sn, contradicting the experimental situation. On the contrary, the AMF correction [Eq. (7)] with moderate U values does not lead to enhanced moments and keeps the picture of NM U_2Fe_2Sn for the experimental lattice intact. In Fig. 8, we show the spin and orbital moments of the U and Fe atoms in U_2Fe_2Sn as functions of Hubbard parameter U. Calculations are performed with the DFT+U method using the AMF correction to the electron potential. The data shown are obtained for the lattice with experimental value of parameter a and $c = 3.5255$ Å. According to Figs. 7(c) and 7(d), the DFT calculations give that for these lattice parameters, the system is close to the transition from FM to NM state.

In Fig. 8, we present the results of two types of calculations. The filled circles and solid lines show the data obtained in the calculations where the DFT+U correction was applied to both U 5f and Fe 3d states. The open circles and dashed lines show the results obtained with the correction applied to the U 5f states only.

We begin with the discussion of the first type of the calculation. Up to U value of ~1.35 eV, there is no substantial enhancement of the atomic moments and the DFT picture of the system remains valid. The values of the spin moments of the U and Fe atoms are very close to each other. The value of the U orbital moment is somewhat smaller than the

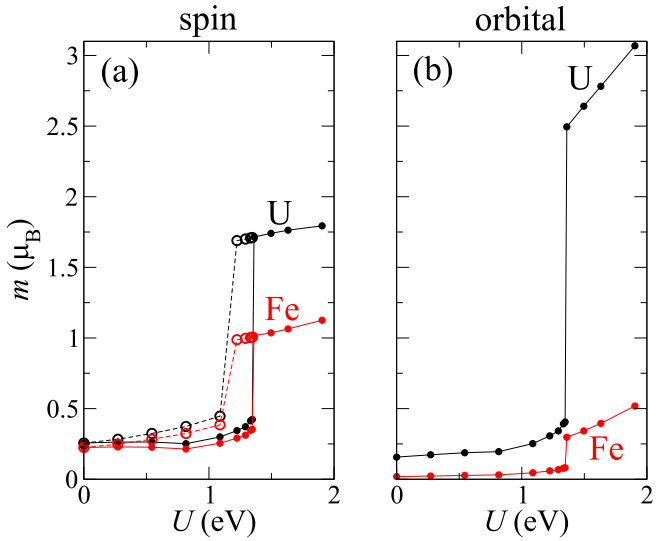

FIG. 8. Spin and orbital moments of the U and Fe atoms in U_2Fe_2Sn as functions of Hubbard parameter U. Calculations are performed with the DFT+U method using the AMF double counting correction to the electron potential. The data shown are obtained for the lattice with experimental value of parameter a and $c = 3.5255$ Å. According to Figs. 7(c) and 7(d), the DFT calculations give that for these lattice parameters the system is close to the transition from FM to NM state. The data shown with filled circles and solid lines are obtained in the calculations where DFT+U correction was included for both U 5f and Fe 3d electrons. The calculations with the correction included only for the U 5f electrons (empty circles, dashed lines) give qualitatively similar results.

value of the U spin moment. For larger U values, U_2Fe_2Sn discontinuously transforms to the state with large spin and orbital moments of the U atoms. Now the U spin moment is distinctly larger than the Fe spin moment and the U orbital moment is larger than the U spin moment. In this U region, there is strong enhancement of the U orbital moment with increasing U whereas the value of the U spin moment changes only weakly. On the basis of these features, we draw the conclusion that at $U \sim 1.35$ eV the localization of the U 5f states increases discontinuously.

The calculation with the DFT+U correction applied to the U 5f states only give qualitatively similar results [Fig. 8(a)]. There are some quantitative differences: somewhat larger values of moments in the low-U region and the shift of the discontinuity point to $U \sim 1.2$ eV. These results show that, expectantly, the DFT+U correction for the U 5f states has a distinctly stronger effect on the properties of the U-based systems than the correction for the Fe 3d states.

The DFT+U calculations with moderate U values and the AMF form of the double-counting correction support the qualitative picture obtained in the DFT calculations. Since the DFT picture agrees in important respects with the experiment, it is of high interest to perform the DFT calculations for the mixed hydrogenated systems aiming to establish how the properties obtained for the parent systems are reflected in the properties of the systems with mixed chemical composition. These results are presented in the next section.

E. Hydrogenated $U_2(Ni_{1-x}Fe_x)_2Sn$ systems

Next we will consider hydrogenated $U_2(Ni_{1-x}Fe_x)_2Sn$ systems. We perform calculations for x equal to 0.25, 0.5, 0.75, and 1.0. The lattice parameters for various x values can be found in Ref. [17]. For values of x not given in Ref. [17], we performed linear interpolation between the closest x points. We consider one H atom per one U atom [24]. The experiment [24] suggests that the positions of the H atoms deviate by 0.127 Å from the planes of the U atoms (Fig. 1).

Our goal is to verify if the conclusions drawn above are operative in the case of these systems, namely, does the substitution of Ni atoms by Fe atoms produce the trend to the replacement of the AFM ground state by the FM ground state associated with the appearance of large spin moments at the Fe sites?

There is no experimental information about the microscopic distribution of the Fe and Ni atoms in the mixed materials. In the calculations, we restrict ourselves to the study of systems with periodicity coinciding with the periodicity of the parent compounds. Therefore, for each x value, we need to distribute four Fe and Ni atoms over four positions of the T atoms (Fig. 1). In the case of $x = 0.25$, all four possible positions of the only Fe atom result in equivalent crystal states. The same is true for $x = 0.75$ and the four positions of the only Ni atom. In the case of $x = 0.5$, there are two inequivalent possibilities: two Fe atoms can be either at positions 1 and 3 or at positions 1 and 2.

For each x value, we performed calculations for three magnetic configurations of the U atoms: AFM-A, AFM-G, and FM (Fig. 4). In Table II, we present for all x values and all magnetic structures spin and orbital moments of the U and T (T = Ni,Fe) atoms, total moment per one U atom, and total energy per one U atom counted from the energy of the FM state. Since for $x = 0.5$ there are two inequivalent distributions of the Fe and Ni atoms over available T atomic positions, we performed FM calculations for both cases. In the table, these two cases are denoted as FM and FM-1. Also, for $x = 0.5$, we performed calculations of the FM structure with atomic moments collinear to the x axis (denoted in Table II as FM100).

The analysis of Table II allows us to formulate a number of conclusions. (i) The values of the U spin and orbital moments depend, for all x values, on the magnetic structure of the U subsystem. The moments are smallest for the AFM-A structure and largest for the FM structure. (ii) The Ni moments are very small in all cases studied. A large Fe spin moment is obtained only for the FM structure of the U sublattice. (iii) A sizable total moment is obtained only for the FM structure. Small total moments of the AFM-A structures are the result of the inequivalence of the U atoms leading to uncompensated antiferromagnetism. In the AFM-G structure, neighboring U layers compensate each other exactly. (iv) In all cases, the FM state has the lowest energy. The energy difference between the FM structure and AFM-G structure, that is, the ground state of the unhydrogenated U_2Ni_2Sn, is small for $x = 0.25$ and increases strongly with increasing Fe content. (v) Calculations for the FM100 structure with atomic moments collinear to the x axis show an increase of energy with respect to the corresponding FM structure with moments collinear to the

TABLE II. Atomic spin and orbital magnetic moments, total magnetic moments, and energies of hydrogenated $U_2(Ni_{1-x}Fe_x)_2Sn$ for a number of x values. For each x value, three magnetic structures of the U subsystem are considered: AFM-A, AFM-G, FM. For $x = 0.5$, there are two inequivalent distributions of the Fe and Ni atoms over four available T atomic positions (cases FM and FM-1 in the table). Also for $x = 0.5$, we performed calculation with atomic moments collinear to the x axis (case FM100). The energy of the FM state is used as an energy origin. For $x = 1$, the AFM-A configuration converges to the nonmagnetic state with zero atomic moments. Numbering of the U and T atoms is according to Fig. 1.

		U_1	U_2	U_3	U_4	T_1	T_2	T_3	T_4	m_{tot}	E
						(μ_B)				(μ_B/U)	(eV/U)
						$x = 0.25$					
						Fe	Ni	Ni	Ni		
AFM-A	spin	0.94	–1.39	1.58	–1.39	0.22	0.02	–0.03	0.02		
	orbit	–1.36	1.95	–2.22	1.95	0.01	0.00	–0.01	0.00		
										0.08	0.019
AFM–G	spin	1.36	–1.47	1.63	–1.47	0.04	0.00	0.01	0.00		
	orbit	–1.86	2.09	–2.31	2.09	0.00	0.00	0.00	0.00		
										0	0.004
FM	spin	1.54	1.52	1.54	1.52	–0.83	–0.04	–0.05	–0.04		
	orbit	–1.97	–2.11	–2.31	–2.11	–0.10	–0.02	–0.01	–0.02		
										0.87	0
						$x = 0.5$					
						Ni	Fe	Ni	Fe		
AFM-A	spin	1.05	–1.06	1.05	–1.06	–0.01	–0.08	–0.01	–0.08		
	orbit	–1.45	1.40	–1.45	1.40	0.00	0.00	0.00	0.00		
										0.075	0.025
AFM–G	spin	1.22	1.31	1.22	1.31	0.00	–0.05	0.00	–0.05		
	orbit	–1.65	1.70	–1.65	1.70	0.00	0.00	0.00	0.00		
										0.0	0.011
FM	spin	1.48	1.53	1.48	1.53	–0.01	–0.84	–0.01	–0.84		
	orbit	–1.86	–1.81	–1.86	–1.81	–0.01	–0.10	–0.01	–0.10		
										0.81	0
FM100	spin	1.38	1.45	1.38	1.45	–0.01	–0.90	–0.01	–0.90		
	orbit	–1.61	–1.70	–1.61	–1.70	0.00	–0.12	0.00	–0.12		
										0.75	0.011
						Ni	Ni	Fe	Fe		
FM–I	spin	1.48	1.48	1.43	1.43	–0.02	–0.02	–0.83	–0.83		
	orbit	–2.03	–2.03	–1.64	–1.64	–0.01	–0.01	–0.09	–0.09		
										0.86	>0.001
						$x = 0.75$					
						Fe	Fe	Fe	Ni		
AFM-A	spin	0.60	–0.09	0.60	–1.06	0.03	–0.10	0.03	0.03		
	orbit	–0.80	0.12	–0.80	1.54	0.00	–0.01	0.00	–0.00		
										0.01	0.026
AFM-G	spin	1.00	–0.78	1.00	–1.19	–0.02	–0.02	–0.02	0.00		
	orbit	–1.35	1.02	–1.35	1.68	0.00	–0.00	0.00	–0.00		
										0	0.017
FM	spin	1.38	1.31	1.38	1.35	–0.79	–0.77	–0.79	–0.00		
	orbit	–1.52	–1.40	–1.52	–1.69	–0.10	–0.09	–0.10	–0.01		
										0.82	0
						$x = 1$					
						Fe	Fe	Fe	Fe		
AFM-A	spin	0.00	0.00	0.00	0.00	0.00	0.00	0.00	0.00		
	orbit	0.00	0.00	0.00	0.00	0.00	0.00	0.00	0.00		
										0	0.012
AFM-G	spin	0.52	0.52	0.52	0.52	0.01	0.01	0.01	0.01		
	orbit	–0.68	–0.68	–0.68	–0.68	0.00	0.00	0.00	0.00		
										0	0.011
FM	spin	0.90	0.90	0.90	0.90	–0.52	–0.52	–0.52	–0.52		
	orbit	–0.98	–0.98	–0.98	–0.98	–0.07	–0.07	–0.07	–0.07		
										0.66	0

z axis. This result correlates with the recent preliminary experimental finding [25]. The atomic moments of the FM100 structure differ somewhat from the atomic moments of the FM structure: the U moments tend to decrease while the Fe moments tend to increase. Importantly, also in the case of the FM100 structure, the FM configuration of the U spin moments is connected with the presence of oppositely directed large Fe spin moments. (vi) The calculations for the two inequivalent distributions of the Fe and Ni atoms over T positions for $x = 0.5$ (cases FM and FM-1) gave very close energies with a difference below 1 meV. Like in point (v), the important relation between FM configurations of the U moments and values and directions of the Fe moments is valid for both FM and FM-1 structures. (vii) These observations suggest that the transition from the AFM ground state to the FM one observed in $U_2(Ni_{1-x}Fe_x)_2Sn$ indeed correlates with the appearance of large spin moments on the Fe sites. The latter appear only in the case of the FM structure of the U moments where the influence of the U spin moments on the Fe spin moments by means of the U-Fe hybridization is maximal.

Above we emphasized the fact that hydrogenation of a U-based system leads to increased lattice parameters and, respectively, to increased distances between U atoms. This, however, is not the only consequence of the H absorption. The H electrons can also participate in chemical bonding and electron density redistribution (see, e.g., Ref. [45]). To isolate the effect of the lattice expansion, we performed calculations for the FM structure of $U_2(Ni_{0.75}Fe_{0.25})_2Sn$ with the lattice parameters of the hydrogenated system but without actual presence of the H atoms. We obtained the increase of the U spin moments from 1.52-1.54 μ_B to 1.83-1.88 μ_B and the increase of the oppositely directed Fe spin moment from 0.83 to 1.26 μ_B. This shows that although qualitative features of the hydrogenation may be captured by the calculation with increased lattice parameters, for obtaining reliable quantitative information the presence of the H atoms must be explicitly taken into account.

IV. CONCLUSIONS

This paper is motivated by the experimental observation of the transformation of the hydrogenated $U_2(Ni_{1-x}Fe_x)_2Sn$ from an AFM state at $x = 0$ to the FM state for $x > 20\%$. The appearance of the ferromagnetism is unexpected since, first, the parent compounds U_2Ni_2Sn and U_2Fe_2Sn are respectively antiferromagnet and Pauli paramagnet and, second, the ferromagnetism is very unusual for the U compounds with the given crystal lattice.

We report systematic theoretical study based on the DFT and DFT+U calculations. The calculation of hydrogen-free parent U_2Ni_2Sn and U_2Fe_2Sn in their experimental lattices give in agreement with experiment the AFM and paramagnetic states, respectively. We demonstrate the dependence of the magnetic state on the variation of the lattice parameters by calculating U_2Fe_2Sn in the lattice of U_2Ni_2Sn and by the investigation for both parent systems the QPTs between NM and magnetic states.

We reveal that a strong difference of the 3d-5f hybridization in the two systems leads to fundamentally different characters of the magnetic states. U_2Ni_2Sn has well-defined U atomic moments and can be mapped on the Heisenberg-type Hamiltonian of interacting U moments. In U_2Fe_2Sn, strong 5f-3d hybridization leads to the Pauli paramagnetism for the equilibrium lattice and contributes to the simultaneous appearance of comparable in value U and Fe spin moments for larger lattice parameters. The calculations show that the presence of the Fe moments is essential for the magnetism of U_2Fe_2Sn. This imposes a constraint on the magnetic structure of the U sublattice: it must be FM. The established correlation between U and Fe spin moments is a decisive factor for understanding the physical nature of the ferromagnetism observed in the hydrogenated $U_2(Ni_{1-x}Fe_x)_2Sn$.

We conclude with the remark that the DFT and DFT+U methods used in the paper do not take into account the quantum dynamical fluctuations that are an important feature of the correlated electron systems. The application of the DMFT approach [46,47], though very demanding in the case of the complex systems studied, would be very desirable to obtain a complete picture of the physics of the U-based compounds.

ACKNOWLEDGMENT

The authors acknowledge financial support of the Czech Science Foundation Project No. 21-09766S.

[1] V. Sechovsky and L. Havela, in *Handbook of Magnetic Materials*, edited by K. H. Bushow (Elsevier, Amsterdam, 1998), p. 1.
[2] P. Santini, R. Lemanski, and P. Erdos, Adv. Phys. **48**, 537 (1999).
[3] J. A. Mydosh, Adv. Phys. **66**, 263 (2017).
[4] S. G. Magalhaes, A. C. Lausmann, E. J. Calegari, and P. S. Riseborough, Phys. Rev. B **101**, 064407 (2020).
[5] J. Willwater, N. Steinki, D. Menzel, R. Reuter, H. Amitsuka, V. Sechovsky, M. Valiska, M. Jaime, F. Weickert, and S. Süllow, Phys. Rev. B **103**, 054408 (2021).
[6] J. A. Mydosh, P. M. Oppeneer, and P. S. Riseborough, J. Phys.: Condens. Matter **32**, 143002 (2020).
[7] D. Aoki, A. Huxley, E. Ressouche, D. Braithwaite, J. Flouquet, J.-P. Brison, E. Lhotel, and C. Paulsen, Nature (London) **413**, 613 (2001).
[8] P. Coleman, Heavy fermions: Electrons at the edge of magnetism, in *Handbook of Magnetism and Advanced Magnetic Materials*, edited by H. Kronmuller and S. Parkin (John Wiley, Chichester, 2007), Vol. 1.
[9] G. Zwicknagl, Rep. Prog. Phys. **79**, 124501 (2016).
[10] G. R. Stewart, Rev. Mod. Phys. **73**, 797 (2001).
[11] A. Miyake, L. M. Sandratskii, A. Nakamura, F. Honda, Y. Shimizu, D. Li, Y. Homma, M. Tokunaga, and D. Aoki, Phys. Rev. B **98**, 174436 (2018).
[12] M. Brando, D. Belitz, F. M. Grosche, and T. R. Kirkpatrick, Rev. Mod. Phys. **88**, 025006 (2016).

[13] S. Maskova, A. V. Andreev, Y. Skourski, S. Yasin, D. I. Gorbunov, S. Zherlitsyn, H. Nakotte, K. Kothapalli, F. Nasreen, C. Cupp, H. B. Cao, A. Kolomiets, and L. Havela, Phys. Rev. B **99**, 064415 (2019).
[14] L. M. Sandratskii, S. Maskova, L. Havela, M. Divis, and K. Carva, Phys. Rev. B **101**, 184433 (2020).
[15] L. M. Sandratskii and L. Havela, Phys. Rev. B **101**, 100409(R) (2020).
[16] S. Maskova-Cerna, A. Kolomiets, J. Prchal, I. Halevy, V. Buturlim, M. Nikolaevsky, O. Koloskova, P. Kozelj, M. König, M. Divis, L. M. Sandratskii, J. Kastil, A. V. Andreev, E. Svanidze, and L. Havela, Phys. Rev. B **103**, 035104 (2021).
[17] S. Maskova, L. Havela, A. Kolomiets, K. Miliyanchuk, A. V. Andreev, H. Nakotte, J. Peterson, Y. Skourski, S. Yasin, S. Zherlitsyn, and J. Wosnitza, J. Korean Phys. Soc. **62**, 1542 (2013).
[18] T. Vojta, Ann. Phys. **512**, 403 (2000).
[19] A. R. Williams, J. Kübler, and C. D. Gelatt, Phys. Rev. B **19**, 6094 (1979).
[20] V. Eyert, *The Augmented Spherical Wave Method*, Lecture Notes in Physics Vol. 849, (Springer-Verlag, Berlin, 2012).
[21] L. M. Sandratskii, Adv. Phys. **47**, 91 (1998).
[22] J. P. Perdew, K. Burke, and M. Ernzerhof, Phys. Rev. Lett. **77**, 3865 (1996).
[23] L. M. Sandratskii, Phys. Rev. B **88**, 064415 (2013).
[24] K. Miliyanchuk, L. Havela, L. C. J. Pereira, A. P. Goncalves, and K. Prokes, J. Magn. Magn. Mater. **310**, 945 (2007).
[25] O. Koloskova (unpublished).
[26] Y. Baer, H. R. Ott, and K. Andres, Solid State Commun. **36**, 387 (1980).
[27] J. Kitagawa and M. Ishikawa, Solid State Commun. **153**, 76 (2013).
[28] V. I. Anisimov, F. Aryasetiawan, and A. I. Lichtenstein, J. Phys.: Condens. Matter **9**, 767 (1997).
[29] S. L. Dudarev, G. A. Botton, S. Y. Savrasov, C. J. Humphreys, and A. P. Sutton, Phys. Rev. B **57**, 1505 (1998).
[30] A. G. Petukhov, I. I. Mazin, L. Chioncel, and A. I. Lichtenstein, Phys. Rev. B **67**, 153106 (2003).
[31] A. B. Shick, A. I. Liechtenstein, and W. E. Pickett, Phys. Rev. B **60**, 10763 (1999).
[32] O. Bengone, M. Alouani, P. Blöchl, and J. Hugel, Phys. Rev. B **62**, 16392 (2000).
[33] V. I. Anisimov, J. Zaanen, and O. K. Andersen, Phys. Rev. B **44**, 943 (1991).
[34] L. M. Sandratskii and K. Carva, Phys. Rev. B **103**, 214451 (2021).
[35] O. Eriksson, M. S. S. Brooks, and B. Johansson, Phys. Rev. B **41**, 7311 (1990).
[36] I. V. Solovyev, A. I. Liechtenstein, and K. Terakura, Phys. Rev. Lett. **80**, 5758 (1998).
[37] P. Mohn, C. Persson, P. Blaha, K. Schwarz, P. Novak, and H. Eschrig, Phys. Rev. Lett. **87**, 196401 (2001).
[38] J. Kübler, *Theory of Itinerant Electron Magnetism* (Oxford University Press, New York, 2002).
[39] T. Moriya, *Spin Fluctuations in Itinerant Electron Magnetism* (Springer, Berlin, 1985).
[40] M. Uhl, L. M. Sandratskii, and J. Kübler, Phys. Rev. B **50**, 291 (1994).
[41] T. Endstra, G. J. Nieuwenhuys, and J. A. Mydosh, Phys. Rev. B **48**, 9595 (1993).
[42] H. H. Hill, *Plutonium and Other Actinides*, edited by W. N. Miner (AIME, New York, 1970).
[43] A. B. Shick, S.-i. Fujimori, and W. E. Pickett, Phys. Rev. B **103**, 125136 (2021).
[44] Since the calculations are performed taking SOC into account, there is no pure spin-up or spin-down states. The states are always spin mixed. Referring to the spin-down or spin-up states, we mean the states where the corresponding spin component is predominant.
[45] I. Tkach, M. Paukov, D. Drozdenko, M. Cieslar, B. Vondrackova, Z. Matej, D. Kriegner, A. V. Andreev, N.-T. H. Kim-Ngan, I. Turek, M. Divis, and L. Havela, Phys. Rev. B **91**, 115116 (2015).
[46] G. Kotliar, S. Y. Savrasov, K. Haule, V. S. Oudovenko, O. Parcollet, and C. A. Marianetti, Rev. Mod. Phys. **78**, 865 (2006).
[47] B. Chatterjee and J. Kolorenc, Phys. Rev. B **103**, 205146 (2021).